3 axis simulator of the Earth magnetic field

João Victor Lopes de Loiola, Letícia Câmara van der Ploeg, Rodrigo Cardoso da Silva, Fernando Cardoso Guimarães, Renato Alves Borges, Geovany Araújo Borges
Department of Electrical Engineering
University of Brasília
Brasília, Brazil-DF 70910-900.
+55 (61) 3107-1040
victor@lara.unb.br, leticiacvdploeg@gmail.com, rcsilva@lara.unb.br, fguimaraes@lara.unb.br, raborges@ene.unb.br, gaborges@unb.br

Simone Battistini, Chantal Cappelletti
Faculty of Gama
University of Brasília
Brasília, Brazil-DF 72444-240.
+55 (61) 3107-8901
simone.battistini@aerospace.unb.br, chantal@aerospace.unb.br

***Abstract*—This work presents the development and implementation of an Earth magnetic field simulator (EMFS) which replicates the magnetic field of the Earth in various points of an orbit by controlling the current that flows through three pairs of coils of a Helmholtz cage. Based on measurements of magnetic field in the main axis of one coil pair and different points of the simulator, it was possible to design a strategy to measure the volume of field uniformity and observe how vectors of magnetic field flow in different points in the cage.**

TABLE OF CONTENTS

1. INTRODUCTION

This work deals with the design and implementation of a magnetic field simulator. This simulator provides controllable magnetic field used to test and validate systems that will operate in space environment. Simulating space conditions on Earth reduces the risk and cost of space missions.

Some configurations of this simulator are commonly found in literature, such as Helmholtz, Merritt and Ruben coils systems [1]. The Helmholtz cage, due to the geometry and the fact that it is composed basically by three pairs of coils, is considered one of the simplest configurations. Although it is simple, it can generate a magnetic field with a satisfactory homogeneity, magnitude and direction. Therefore, this coil system is mainly used in different works. As it was pointed out in [2], a strategy to produce a magnetic field with the desired magnitude and direction is by placing three coils in an orthogonal configuration aligned with x,y, and z axes of a rectangular coordinate system.

978-1-5386-2014-4/18/$31.00

In order to develop systems that consider those space conditions, the Laboratory of Application and Innovation on Aerospace Science (LAICA) from University of Brasilia (UnB) developed a test platform for nanosatellites. This platform is composed of a three degrees of freedom test-bed and a Helmholtz cage. In this paper an implementation of an EMFS using a Helmholtz cage with square coils will be discussed. Based on measurements of the magnetic field in the main axis of one coil pair, it is possible to estimate the volume of the region of field uniformity.

Recent papers present the development of similar Helmholtz cages. In [3], a three axis magnetic field simulator was designed and manufactured using square coil pairs in order to simulate orbital magnetic field and to calibrate magnetic sensors. Other two works where similar Helmholtz cages are presented are [4] and [5]. In both of them a Helmholtz cage constructed with square coil pairs was developed: the first work used the simulator to develop a 3-axis attitude control system using magnetorquers and the second one used the simulator to develop a calibration procedure for triaxial magnetometers.

This paper presents a strategy to measure region of field uniformity and observe how vectors of magnetic field flow in different points in the cage and it is organized as follows: Sec. 2 will present the theory applied to find constructive parameters, Sec. 3 will present the design requirements and the implementations steps taken during EMFS development, Sec. 4 will present the experimental results obtained, and the conclusions will be given in Sec. 5.

2. THEORETICAL BASIS

The Helmholtz cage, named after Hermann Von Helmholtz (1821-1894), consists of three coil pairs placed in an orthogonal arrangement. Such configuration allows the production of a homogeneous magnetic field with desired magnitude and direction. Fig. 1 shows the Helmholtz's cage developed at LAICA, its design specifications were defined considering some theoretical results given in this section.

In order to derive the Helmholtz cage magnetic field equation, only one pair of coils is firstly considered and the results are extended to the other pairs due to symmetry. Fig. 2 shows

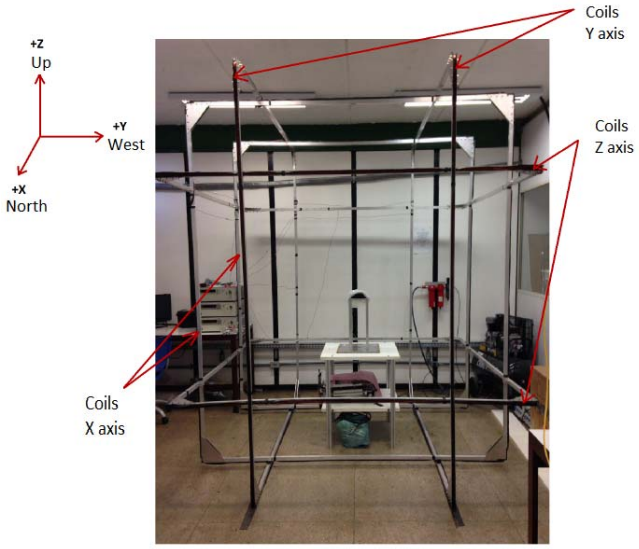

Figure 1. **Helmholtz's cage developed by LAICA/UNB.**

a pair of square coils and an orthogonal frame placed at the center of the coil in the bottom. The magnetic field intensity along z, $B(z)$, can be obtained by Biot-Savart's law. When this law is applied to one side of the coil in the bottom, from points $(-L/2, L/2, 0)$ and $(L/2, L/2, 0)$, for example, it leads to Eq. 1.

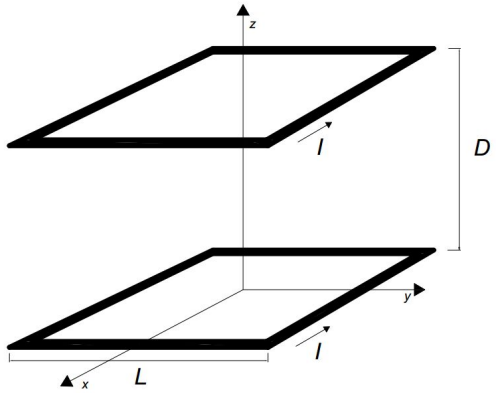

Figure 2. **Coil pair representation in a reference frame.**

$$B_{side}(z) = \frac{\mu_0 NI}{4\pi} \int_{\frac{-L}{2}}^{\frac{L}{2}} \frac{\frac{L}{2}dx}{(z^2 + (\frac{L}{2})^2 + x^2)^{\frac{3}{2}}}, \quad (1)$$

Where $B_{side}(z)$ refers to the magnetic field intensity generated by the side under analysis in the same direction of the z-axis, L is the total length of one side of the square coil, μ_0 is the medium magnetic permeability and I is the electric current. Resolving the integral, the field intensity is given by Eq. 2.

$$B_{side}(z) = \frac{\mu_0 NI}{\pi} \frac{L^2}{(4z^2 + L^2)\sqrt{4z^2 + 2L^2}}, \quad (2)$$

The results shown in Eqs. 1 and 2 are well known and can be seen in [6] and [2]. Using symmetry arguments, the magnetic field produced by the four sides of the coil in the bottom and the four sides of the coil in the top, is given by Eq. 3.

$$B(z) = 4B_{side}(z) + 4B_{side}(D - z) \quad (3)$$

Where D is the distance between the coils. Defining an auxiliary function f, given by Eq. 4, Eq. 3 can be written as in Eq. 5.

$$f(\gamma) = \frac{1}{(\gamma^2 + 1)\sqrt{\gamma^2 + 2}} \quad (4)$$

$$B(z) = \frac{4\mu_0 NI}{\pi L}\left[f\left(\frac{z}{L/2}\right) + f\left(\frac{D-z}{L/2}\right)\right] \quad (5)$$

In order to analyse the homogeneity of the field, the derivatives of $B(z)$ with z must be found. Eq. 6 gives the first order derivative of $B(z)$.

$$\frac{dB(z)}{dz} = \frac{4\mu_0 NI}{\pi L}\left(\frac{2}{L}\right)\left[f'\left(\frac{z}{L/2}\right) - f'\left(\frac{D-z}{L/2}\right)\right] \quad (6)$$

Eq. 6 shows that at the cage center $z = z_0$, where $z_0 = D/2$, the first order derivative of $B(z)$ is zero. However, this result is not sufficient to achieve the desired homogeneity. Since the second order derivative is associated to the concavity of the curves, if its value is zero at $z = z_0$, the field $B(z)$ can be approximated by a constant function within a region centered in z_0. Eq. 7 gives the second order derivative of $B(z)$ and Eq. 8 gives its value in z_0.

$$\frac{d^2B(z)}{dz^2} = \frac{4\mu_0 NI}{\pi L}\left(\frac{2}{L}\right)^2\left[f''\left(\frac{z}{L/2}\right) + f''\left(\frac{D-z}{L/2}\right)\right] \quad (7)$$

$$\frac{d^2B(z_0)}{dz^2} = \frac{8\mu_0 NI}{\pi L}\left(\frac{2}{L}\right)^2\left[f''\left(\frac{D}{L}\right)\right] \quad (8)$$

The second order derivative of f is given by Eq. 9. This equation shows that for a certain value of γ, the second order derivative of $B(z)$ can be zero in z_0.

$$\frac{d^2f(\gamma)}{d\gamma^2} = \frac{2(6\gamma^6 + 18\gamma^4 + 11\gamma^2 - 5)}{(\gamma^2 + 1)^3(\gamma^2 + 2)^{5/2}} \quad (9)$$

Let be γ_{ideal} the value that leads Eq. 9 to zero. The numerical solution shows there is only one real positive value of γ which satisfies such condition. This value is given by $\gamma_{ideal} = 0.544505643$. Since $\gamma = D/L$, which can be seen in Eq. 8, if L is predefined as a design parameter, there is an optimal value of D which allows the generation of a homogeneous magnetic field inside the cage. This optimal value D_{ideal} is given by Eq. 10.

$$D_{ideal} = \gamma_{ideal} L = 0.5445L \quad (10)$$

Theoretical field uniformity for the designed simulator

Based on the ideal γ it is possible to find an optimum relation between D and L. This constant ensures the largest field uniformity in the center of the Helmholtz cage. As it can be seen in Fig. 3, it is considered a limit of 0.05% of tolerance, among all different values for γ, the ideal one had presented the largest field uniformity kept constant from -0.2 to 0.2 meters approximately. For γ with error of $+2\%$ this picture shows that the region of field uniformity has more variation and the maximum field intensity is not in the center. Furthermore, for γ with error of -2% the maximum field intensity is kept in the middle but the region of field uniformity decreases.

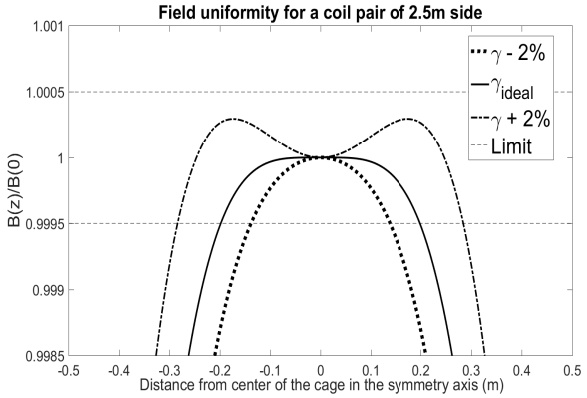

Figure 3. **Theoretical field uniformity simulated for different values of γ**

3. EMFS DESIGN AND IMPLEMENTATION

Design Requirements

The EMFS must take as input a point representing the orbital position of a satellite around the Earth. Orbit points are defined by longitude, latitude and altitude parameters, Earth's magnetic field at those positions can be obtained from publicly available mappings such as the Word Magnetic Model (WMM) provided by [9]. Considering the above general goal, the EMFS must address some specific requirements:

- Generated magnetic field must be sufficiently homogeneous inside a region around the cage center. This region shall be large enough to contain the test-bed and any equipment under test.
- The cage must overcome the environment magnetic fields.
- The system must be able to produce a magnetic field in any direction at the cage center.
- The EMFS capabilities shall simulate the Earth's magnetic field well enough to test nano-satellite technologies such as magnetorquers and attitude determination techniques based on magnetometers.

Therefore, to achieve the specified requisites, the physical prototype was built with parameters shown in Tab. 1.

In Tab. 1, the first column refer to the orthogonal coils pair on each axis, N is the number of turns on each coil, Ω is the resistance of each coil and $Cur.$ refer to the maximum current applied on each coil pair.

Table 1. **Electrical parameters obtained from the physical prototype.**

Pair	N	Len.(m)	Ω	Cur.(A)	Vol.(V)	Pow.(W)
X	20	2.5	6.6±0.1	5.98	40	239.2
Y	20	2.5	6.8±0.1	5.76	40	230.4
Z	20	2.5	6.9±0.1	5.76	40	230.4

DC Power Supplies

Each of the three coil pairs are connected to a programmable DC power supply of the 6032A Agilent model. Each one of the three power supplies, shown in Fig. 4, can provide up to 60V or 50A until the limit of 1000W.

Figure 4. **DC Power Supplies connected to the three coil pairs.**

The power supplies are connected to a single computer through GPIB interfaces. Using the command languages SCPI and ARPS one can program the output voltage or current whilst the power provided is automatically adjusted by autorange feature.

The environment used to program the power supplies is MATLAB, which is convenient to integrate orbit inputs to magnetic field outputs by means of WMM databases and equation fields described earlier. Details about EMFS software are explained in the next topic.

EMFS Software

MATLAB works as an unified simulation environment for EMFS, it has the Instrument Control Toolbox, which allows communication between a computer and GPIB instruments, and the **wrldmagm** function. The later is based in WMM databases updated every 5 years, since the Earth's magnetic field changes with time. The current WMM (WMM-2015) period began at January 1st, 2015.

MATLAB **wrldmagm** function take as inputs the altitude, latidude and longitude information besides the year when simulation is performed. WMM model predicts magnetic field behavior within the 5-year period, describing only the long-wavelength portion of the Earth's internal magnetic field though. Such long-wavelength portion is primarily generated by the planet outer core, whereas the portions generated by Earth's crust and upper mantle, and by the ionosphere, and magnetosphere are not well represented [10].

The outputs of **wrldmagm** function are the Earth's magnetic field as a vector object of MATLAB environment, the field horizontal intensity, a declination angle, an inclination angle,

and the field total intensity. Having the field vector, EMFS software calculates the electric currents the power supplies must provide using Eq. 6. Therefore, only the vector object output is used.

The SCPI commands currently implemented allow only the output voltages of the power supplies to be set up. Since the cage magnetic field depends directly of the electric currents which flow through the coil pairs, the relationship between the currents and applied voltage had to be found. Experiments performed led to Eqs. 11 to 13, which state the relationship between the output voltage (V) and output current (I) for each coil pair, indexed accordingly to directions x, y and z. Fig. 5 shows the voltage-current curves encountered.

$$V_x = \frac{I_x - 0.0156}{0.1522} \tag{11}$$

$$V_y = \frac{I_y - 0.0133}{0.1449} \tag{12}$$

$$V_z = \frac{I_z - 0.0077}{0.1460} \tag{13}$$

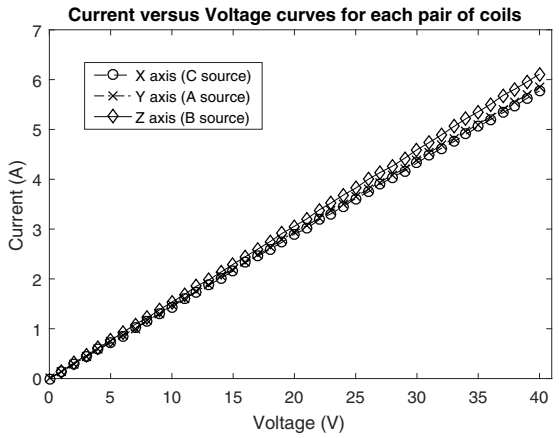

Figure 5. **Voltage-current relationship for each load (coil pairs) connected to the power supplies.**

The whole procedure realized under MATLAB environment consists of defining the orbit trajectory, sending the position data to the **wrldmagm** function, calculating the output currents and voltage, and creating VISA objects that are associated to the Agilent power supplies through their physical address, which allows the SCPI commands to be sent to them. Fig. 6 shows a flowchart that summarizes the software steps. Additionally, it should be mentioned the EMFS works as an open-loop system by now and the future improvements include closing the loop, using three-axis magnetometers and control algorithms.

Experimental procedure

In this work, two procedures were developed for measuring the field uniformity inside the cage. As it will be explained in Sec. 4, one of these experiments consists in measuring the magnetic field inside the cage with the sensor that is embedded in the nanosatellite simulator. In this case, only a $50 \times 50cm$ area is analyzed, since this area is sufficient to cover the nanosatellite simulator and is compatible with

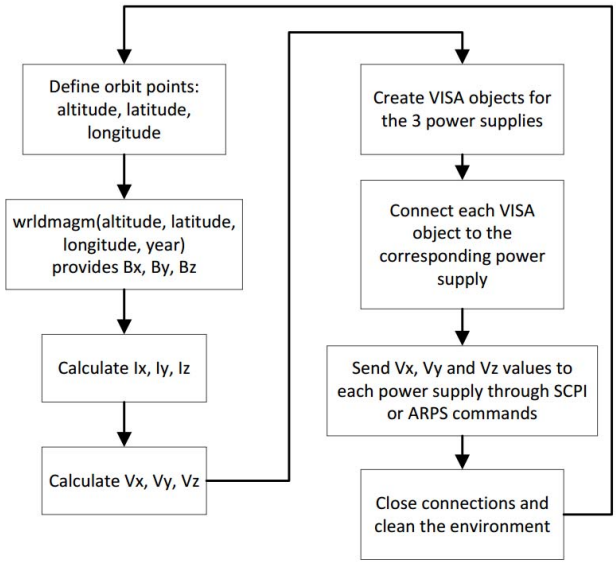

Figure 6. **Flowchart for the EMFS software.**

CubeSat dimensions (up to 3U CubeSats). Further details on this simulator may be verified in [8].

The other procedure, designed to be even more precise, utilizes the HMR2300 sensor, a robust 3-axis magnetometer [7]. This procedure, illustrated by Figs. 7 and 8, can be summarized as follows:

1. The center of the cage and another midway points of the cage are determined.
2. An approximately two meters long plank is positioned in the center of the cage, aligned with its y-axis. This plank is suspended with three string loops, one in each extremity of the plank and one in its middle.
3. This plank is marked with 2cm spaced lines. It is relevant to notice that this can be considered as the measurement error ($\pm 2cm$) provided by the "instrument" scale.
4. The HMR2300 magnetometer is positioned in each of these marks with its axes aligned with those of the cage. Measurements are taken along the whole y-axis of the cage, while inside the cage. Observation: although the computer is depicted in Fig. 8 near the HMR2300 sensor, the caution to hold it as distant as possible from the sensor during the experiment was taken.

4. RESULTS

This section may be divided in the following three experiments:

- Experiment 1: The field uniformity is analyzed with the LSM303 sensor, which is employed in the nanosatellite simulator. The influence of field generation in one axis to the others is also addressed.
- Experiment 2: The field uniformity is further analyzed in the y-axis of the cage with the aid of a more robust magnetometer (HMR2300).
- Experiment 3: a brief experiment is made in order to verify the magnetic field vector inside the cage in specific points of it.

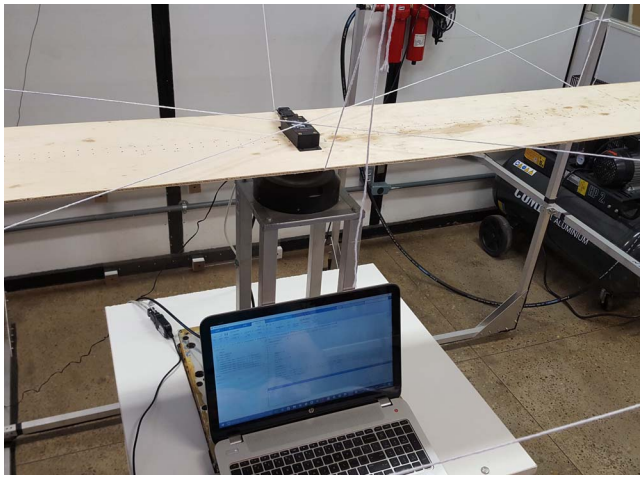

Figure 7. Field uniformity experiment. Measurements are sent from the HMR2300 sensor to a computer.

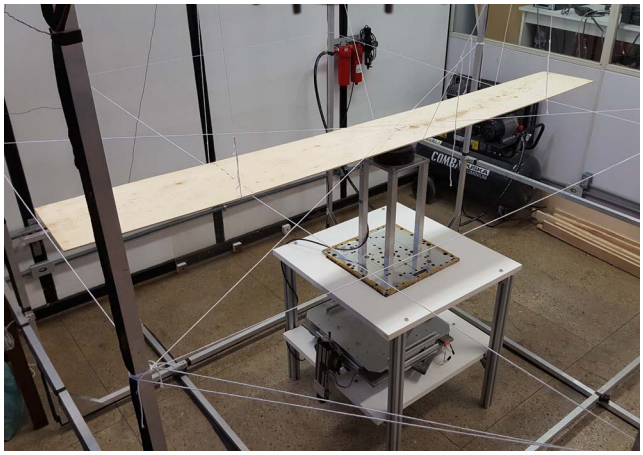

Figure 8. Strings placed along the cage.

Experiment 1 and initial considerations

The simulator is capable of receiving an orbit position and providing the associated magnetic field in the center of the Helmholtz cage. To verify the operation of the simulator, a magnetometer (LSM303 chip) was used. With the readings of the magnetic field in each axis, it is possible to verify the influence of the generation of magnetic field in one axis to the others, *i.e.* how much a specific axis can generate magnetic field in undesired directions. Also, the uniformity of the magnetic field where the nanosatellite platform stands may be verified in terms of norm and direction of the magnetic field vector.

A positive value of magnetic field generation may be applied in each axis to perform the analysis. The chosen value for these tests was $20\mu T$. In a first moment, the value of the environmental magnetic field in the laboratory is determined with all the electric sources turned off. In other words, the magnetic field of the Earth is determined at the center of the cage. The following values were obtained: $B_{LAB,X} = 22,6781\ \mu T$, $B_{LAB,Y} = -7.6950\mu T$ and $B_{LAB,Z} = 13,3681\mu T$.

The adopted procedure was to perform four tests: in three of them, only one pair of coils receives the command to generate $20\mu T$, making possible to verify the influence of the field of one axis in the others; and in the last one, all the three pair of coils receives the command to generate $20\mu T$.

Table 2. Measured magnetic field values at the center of the cage when a $20\mu T$ generation command is sent.

$B_{generated}(\mu T)$			$B_{measured}(\mu T)$		
x	y	z	x	y	z
20	0	0	43.2369	-9.6544	14.0362
0	20	0	22.8706	11.9888	13.2256
0	0	20	22.9606	-9.6037	33.9300
20	20	20	42.7912	12.3106	34.7706

The correct field generation is verified, since the resultant magnetic field is obtained by the sum of the environmental magnetic field and the generated magnetic field ($20\mu T$) in the X, Y and Z axes of the cage. The percent error between the desired magnetic field generation and the measured magnetic field generation was 1,3093%, 2,5696% and 1,6839% in the X, Y and Z axes, respectively. Applying $20\mu T$ in each of the axes simultaneously (see last line of Tab. 2), the obtained percent errors were 0,2650%, 0,0455% and 4,2031% for the X, Y and Z axes, respectively. Some causes to these percent errors may be the possible electromagnetic interference in the laboratory, the influence of magnetic field generation of one axis in the other two axes, the precision of the measurement device and the voltage/current oscillation in each electric source.

To determine if the region occupied by the air bearing table has uniform magnetic field, the values of the B_X and B_Y magnetic fields were verified, taking into consideration that the point 11cm above the air bearing base was arbitrarily chosen as the $(x, y, z) = (0, 0, 0)$ coordinate. The measurements were taken in a $56,5cm \times 56,5cm$ rectangular base with gaps of 2cm between each measurement in both directions (x and y). This limit was chosen taking into account that the air bearing platform has a $50cm \times 50cm$ retangular surface, *i.e.* the measurement range covers all this surface with a certain error margin. It must be remembered that the air bearing platform has an inclination limit, which means that field uniformity analysis in the Z axis would need a lesser range. The uniformity of the *modulus* of the magnetic field in the center of the cage region is illustrated by Fig. 9. The bigger discrepancy between the desired and the obtained magnetic fields was $3,57\mu T$ in the $(x, y, z) = (0, 12, 0)$ point.

Experiment 2: field uniformity with the HMR2300 sensor

As explained earlier in Section 3, an experimental apparatus was prepared in order to evaluate the real field uniformity of the cage. As in the previous experiment, performed with the LSM303 sensor, the magnetic field of the laboratory must be determined before running the experiment. Fig. 10 shows the measurements of magnetic field in the center of the cage when all pairs of coils are turned off.

Then, the magnetic field uniformity experiment explained in Section 3 is performed in the y-axis of the cage with the HMR2300 magnetometer and this pair of coil running at its maximum nominal current. Fig. 11 shows the obtained measurements. A first conclusion is that, since the laboratory magnetic field in this axis is approximately $-1.82\mu T$, the total field variation was about $140\mu T$.

To evaluate if this total field variation is enough to perform

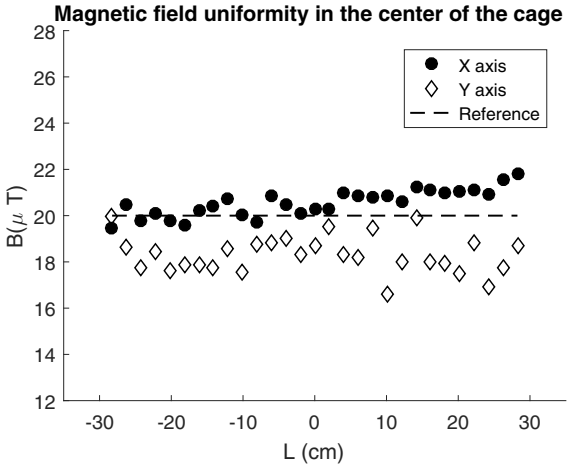

Figure 9. **Variation of the magnetic field in the center of the Helmholtz cage along the symmetry axis of the x and y axes.**

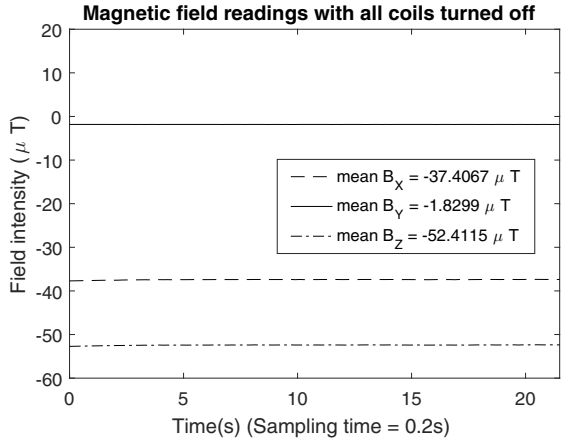

Figure 10. **Magnetic field measurements taken at the center of the cage with all coils turned off.**

orbit experiments, the intensity of the magnetic field of Earth must be known at least in a specific altitude. Fig. 12 shows the magnetic field of Earth at an altitude of 100 kilometers. As it can be seen in this picture, the maximum magnetic field verified is around $65\mu T$, which means that, considering all pairs of coils have similar construction parameters, the proposed magnetic field simulator is capable of simulating any orbit with this altitude or higher.

Furthermore, Fig. 11 shows that in an extension of about one meter the field inside the cage is uniform, given some variation tolerance.

Experiment 3: field vector direction

In this brief experiment, the HMR2300 sensor was placed in 27 different points while the y-axis pair of coils was running with its maximum nominal current. These points form a parallelepiped volume with $2.5m \times 2.5m$ XY base and a $1.3m$ Z height centered with the cage. Since the sensor is held manually in these points, little variation with the magnetic field vector may occur. Also, the real position of this vector are approximations, since they were determined visually. Figs. 13 and 14 show the obtained result. To obtain the vectors illustrated in these pictures, the environmental

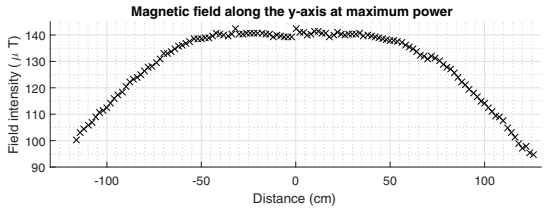

Figure 11. **Magnetic field uniformity in the y-axis of the cage.**

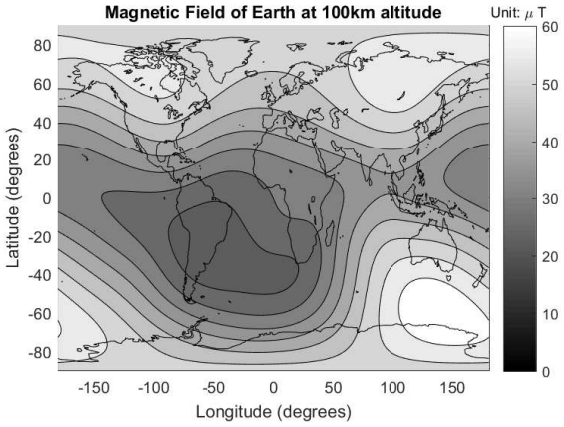

Figure 12. **Intensity of the magnetic field of Earth.**

magnetic field determined in Fig. 10 was subtracted, aiming to represent the magnetic field generated only by the y-axis pair of coils.

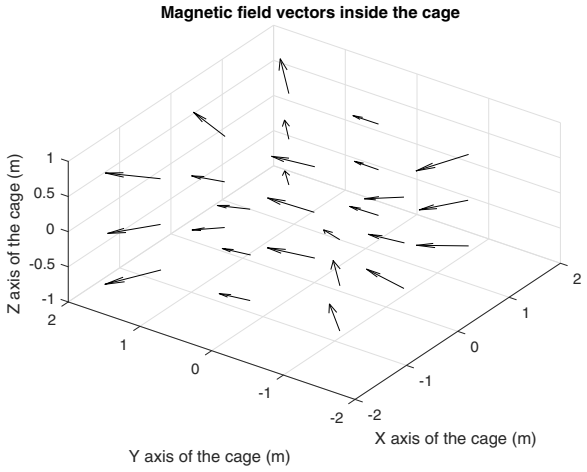

Figure 13. **Magnetic field vectors inside the cage considering only the field generation of the y-axis pair of coils (3D).**

As it can be seen, the magnetic field behaviour is as expected: magnetic field vectors enter in the first coil and exit from the second coil, certifying that both coils generates field in the same direction.

5. CONCLUSIONS

The implementation of the simulator implies the establishment of a didactic environment which makes possible the re-

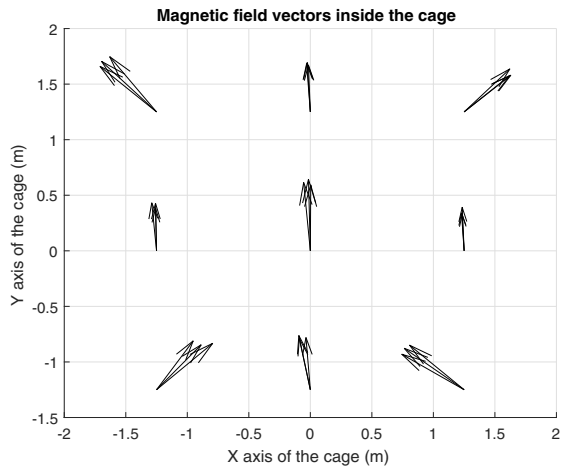

Figure 14. **Magnetic field vectors inside the cage considering only the field generation of the y-axis pair of coils (Upper view).**

alization of experiments and projects of magnetic controllers involving magnetic field alignment. The proposed simulator was developed in a way that the applied voltages on the electric sources are controlled remotely using MATLAB and the results shown in this work indicates that this simulator is adequate for orbit simulations.

ACKNOWLEDGMENTS

This work was supported by the University of Brasília, the Federal District Research Support Foundation (FAPDF) and the Coordination for the Improvement of Higher Education Personnel (CAPES).

REFERENCES

[1] S. M. Adame, J. C. O. Galvan, E. C. Littlewood, R. E. Perez, and E. B. Brisset, Coil Systems to Generate Uniform Magnetic Field Volumes, in Excerpt from the proceedings of the COMSOL conference, Oct 2010.

[2] Batista, D.S.,Granziera, F., Tosin, M.C.,2017. Three-axial Helmholtz Coil Design and Validation for Aerospace Applications. IEEE Transaction on Aerospace and Electronic Systems.DOI 10.1109/TAES.2017.2760560.

[3] F. Piergentili, G. P. Candini, and M. Zannoni, Design, manufacturing, and test of a real-time, three-axis magnetic field simulator, IEEE Transactions on Aerospace and Electronic Systems, vol. 47, no. 2, pp. 13691379, April 2011.

[4] P. G. Haddox, The Development of a Hardware-in-the-Loop Attitude Determination and Control Simulator for IlliniSat-2, in 52nd Aerospace Sciences Meeting, ser. AIAA SciTech. Reston, Virginia: American Institute of Aeronautics and Astronautics, jan 2014.

[5] A. Zikmund, M. Janosek, M. Ulvr, and J. Kupec, Precise calibration method for triaxial magnetometers not requiring earths field compensation, IEEE Transactions on Instrumentation and Measurement, vol. 64, no. 5, pp. 12421247, May 2015.

[6] Lee, S.G., Kang, C.S. and Chang, J.W., 2007. Square loop coil system for balancing and calibration of second-order SQUID gradiometers. IEEE Transactions on applied superconductivity, 17(2), pp.3769-3772.

[7] HMR2300 magnetometer datasheet. Honeywell Inc. Available at: https://aerocontent.honeywell.com/aero/common/documents/myaerospacecatalog-documents/Missiles-Munitions/HMR2300.pdf.

[8] R. C. da Silva, U. A. Rodrigues, R. A. Borges, S. Battistini, C. Cappelletti, B. T. Popov, S. G. P. Costa, P. Beghelli and M. Sampaio. A testbed for attitude determination and control of spacecrafts. In: II IAA Latin American Cubesat Workshop, 2016, Florianópolis. Proceedings of the II IAA Latin American Cubesat Workshop, 2016.

[9] National Centers For Environmental Information. The World Magnetic Model. Available at: https://www.ngdc.noaa.gov/geomag/WMM/DoDWMM.shtml [Online, last access October 14, 2017].

[10] National Centers For Environmental Information. The World Magnetic Model - Accuracy, limitations, magnetic poles and error model. Available at: https://www.ngdc.noaa.gov/geomag/WMM/limit.shtml [Online, last access October 14, 2017].

BIOGRAPHY

João Victor Lopes de Loiola *received the B.S. degree in Electrical Engineering from Federal University of Piauí (UFPI) in 2015. He is currently a M.S. degree student of the Postgraduate Program of Electronic Systems and Automation (PGEA) at UnB. His research interests include optimal filtering, adaptive control and aerospace systems.*

Letícia Câmara van der Ploeg *received the B.S. degree in Mechatronics Engineering from University of Brasília (UnB) in 2017. Her research interests include magnetic field uniformity and aerospace systems.*

G.A. Borges *is professor at Electrical Engineering Department of University of Brasilia. He has a PhD in robotics at LIRMM, Montpellier, France, 2002. He has spent a sabbatical with MERS Team of MIT's Aeroastro Department, 2012. His research interests include aerospace systems, robotics, control systems, stochastic filtering and biomedical engineering.*

Rodrigo Cardoso da Silva *received the B.S. degree in Mechatronics Engineering from University of Brasília (UnB) in 2015. He is currently a M.S. degree student of the Postgraduate Program of Electronic Systems and Automation (PGEA) at UnB. His research interests include nonlinear and adaptive control, aerospace systems, optimal filtering and Lyapunov theory.*

Fernando Cardoso Guimarães *Received his B.S. degree in Mechatronics Engineering from the University of Brasilia in 2014. After working 2 years as an embedded systems development engineer, he began a Masters Degree program at University of Brasilia with focus in aerospace technologies for small satellites. He is affiliated with the Laboratory of Automation and Robotics (LARA) and with the Laboratory of Aerospace Science and Innovation (LAICA) at the same university. His main research interests are embedded systems applied to aerospace technologies, spacecraft guidance, navigation and control, Lyapunov stability theory, robust control, stochastic modeling and filtering.*

Renato Alves Borges *received a Master (2004) and Doctoral (2009) degree in Electrical Engineering from the University of Campinas and a PhD degree in Electrical Engineering from the University of New Mexico (USA) (2009). From 2009 to 2011 he held a post-doctoral fellowship from the state of Sao Paulo Research Foundation working at the School of Electrical and Computer Engineering at the University of Campinas. He is currently an assistant professor in the Electrical Engineering Department of the University of Braslia and a control system researcher affiliated with the Laboratory of Automation and Robotics (LARA) and the Executive Coordinator the Laboratory for Application and Innovation in Aerospace Sciences (LAICA) at the University of Brasilia. His main research interests are Lyapunov stability theory, stability analysis of linear and nonlinear systems, modeling and control of rotating body, dynamic system analysis under uncertainty, and development of high altitude scientific platforms.*

Simone Battistini *received his BSc (2006) and MSc (2009) degrees in Control System Engineering from Sapienza Università di Roma (Italy). He obtained a PhD in Aerospace Engineering (2013) at the Scuola di Ingegneria Aerospaziale, Sapienza Università di Roma. In 2012 he was a visiting researcher at the Faculty of Aerospace Engineering, Technion - Israel Institute of Technology (Israel). In 2017 he was a visiting professor at the Departamento de Enxeñería Mecánica, Máquinas e Motores Térmicos e Fluidos, Universidad de Vigo (Spain). Since 2013, he is an assistant professor in the Aerospace Engineering course at Faculdade Gama, Universidade de Brasília (Brazil) where he is associated with the Laboratory of Aerospace Science and Innovation (LAICA). His main research interests are related with guidance, navigation and control of aerospace vehicles.*

Chantal Cappelletti *received her BSc (2005) in Aerospace Engineering from Sapienza Universtà di Roma and her MSc (2008) in Astronautical Engineering and her PhD (2012) in Aerospace Engineering from the Scuola di Ingegneria Aerospaziale della Sapienza Universita di Roma. Member of International Academy of Astronautics, she is currently an Assistant Professor at University of Brasília. She lead 6 satellite projects from Italy (UNISAT program and others) and from Brazil (SERPENS), she was PI of 2 missions concerning cancer cells behaviour in space and she was an ASI delegate at IADC. She is associated with the Laboratory of Aerospace Science and Innovation (LAICA) of Universidade de Brasília and cofounder of GAUSS Srl. Her main research interests are related with Small Satellites, Biomedical Research in space, Space Debris, Astrodynamics and Attitude Control.*